Geophysical Research Letters

RESEARCH LETTER
10.1029/2021GL097191

Key Points:

- Consistent, western ice sheet margin retreat at ~18–16 ka driven by destabilization due to sea level rise and/or ocean warming
- Retreat stabilized during ~17–13 ka after reaching present coast
- Ice sheet margin may have thinned before ~13 ka, consistent with interior but without substantial marginal retreat

Supporting Information:

Supporting Information may be found in the online version of this article.

Correspondence to:

C. M. Darvill,
christopher.darvill@manchester.ac.uk

Citation:

Darvill, C. M., Menounos, B., Goehring, B. M., & Lesnek, A. J. (2022). Cordilleran Ice Sheet stability During the Last Deglaciation. *Geophysical Research Letters*, *49*, e2021GL097191. https://doi.org/10.1029/2021GL097191

Received 23 NOV 2021
Accepted 5 APR 2022

Author Contributions:

Conceptualization: C. M. Darvill
Formal analysis: C. M. Darvill, B. Menounos, B. M. Goehring
Funding acquisition: C. M. Darvill
Investigation: C. M. Darvill, B. Menounos, B. M. Goehring
Methodology: C. M. Darvill, B. Menounos, B. M. Goehring
Resources: A. J. Lesnek
Visualization: C. M. Darvill
Writing – original draft: C. M. Darvill
Writing – review & editing: B. Menounos, B. M. Goehring, A. J. Lesnek

Cordilleran Ice Sheet Stability During the Last Deglaciation

C. M. Darvill[1], B. Menounos[2,3], B. M. Goehring[4], and A. J. Lesnek[5]

[1]Department of Geography, The University of Manchester, Manchester, UK, [2]Geography, Earth and Environmental Sciences and Natural Resources and Environmental Studies Institute, University of Northern British Columbia, Prince George, BC, Canada, [3]Hakai Institute, Heriot Bay, BC, Canada, [4]Department of Earth and Environmental Sciences, Tulane University, New Orleans, LA, USA, [5]School of Earth and Environmental Sciences, Queens College, CUNY, Queens, NY, USA

Abstract We report 20 ^{10}Be exposure ages from glacial erratics and bedrock on the west coast of British Columbia, Canada, which add to existing chronologies of Cordilleran Ice Sheet retreat along ~600 km of coastal North America. Collectively, these data show the western ice limit reached the present coast by 18–16 ka then retreat slowed for ~4,000 years until 14–13 ka. We attribute initial retreat to destabilization and grounding line retreat resulting from rising sea level and/or ocean warming in the northern Pacific. Subsequent stability of the ice sheet at the present coastal margin was likely due to the transition from marine to terrestrial margins despite increasing temperatures that may have driven ice sheet thinning. Our findings demonstrate the importance of understanding both climatic and nonclimatic drivers of ice sheet change through time.

Plain Language Summary The Cordilleran Ice Sheet once covered western North America and was similar in size and characteristics to the modern Greenland Ice Sheet. It is therefore a good analog for how the Greenland Ice Sheet may respond to changing climate and underlying topography in the future. We show the western margin of the Cordilleran Ice Sheet retreated rapidly from around 18,000 years ago but then stabilized for several thousand years close to the present coastline. Ice may still have been lost during this period of relative stability, but through vertical thinning rather than lateral retreat, demonstrating the importance of understanding ice sheets in three-dimensions. Our reconstruction shows that atmospheric and oceanic temperatures and underlying topography can all control ice sheet stability. We also show that hundreds of kilometers of coastline were free of ice prior to an important period of early human migration into the Americas.

1. Introduction

The nature and rates of past ice sheet response to abrupt climate change provide analogs for how quickly the Greenland and Antarctic ice sheets could respond to changing atmospheric temperatures and warming and rising oceans in the future (Masson-Delmotte et al., 2021; Stokes et al., 2015). The Cordilleran Ice Sheet in western North America was of comparable size and topographic configuration to the modern Greenland Ice Sheet (Figures 1a and 1b) and exhibited similar dynamics, with ice streams channeling rapid flow and a western margin terminating in both marine and terrestrial environments (Eyles et al., 2018; Shaw et al., 2020). Unlike Greenland, the contemporary footprint of the Cordilleran Ice Sheet is exposed, permitting reconstruction of complete deglaciation from geomorphological evidence. Deglacial ocean warming of ~4–8°C in the western Pacific (Taylor et al., 2014) was similar to high-end scenarios for future ocean warming (Masson-Delmotte et al., 2021). Consequently, the deglacial record of the Cordilleran Ice Sheet is an ideal candidate for empirical reconstructions against which to test ice sheet models and determine the response of ice sheets to climate forcing.

Recent studies refined the timing of Cordilleran ice retreat from the continental shelf to the present coastline (Figure 1c). Marginal retreat from Calvert Island (Darvill et al., 2018), Southeast Alaska (Lesnek et al., 2018, 2020), and Haida Gwaii (Mathewes & Clague, 2017) occurred earlier than other margins such as the Puget Lobe (Darvill et al., 2018; Porter & Swanson, 1998). These refinements have implications for the viability of an ice-free coastal human migration route into the Americas during deglaciation, prior to an alternative, interior route (Figures 1a and 1b; Becerra-Valdivia & Higham, 2020; Bennett et al., 2021; Clark et al., 2022; Froese et al., 2019; Potter et al., 2017, 2018; Waters, 2019). However, the precise roles of atmospheric warming, oceanic warming, or sea level rise in controlling ice recession remain less clear. During later stages of deglaciation, the central Cordilleran Ice Sheet may have thinned markedly in response to abrupt climate change, contributing ~2.5–3.0 m to sea level rise (Gomez et al., 2015; Gregoire et al., 2012, 2016; Menounos et al., 2017). Further constraints are needed to

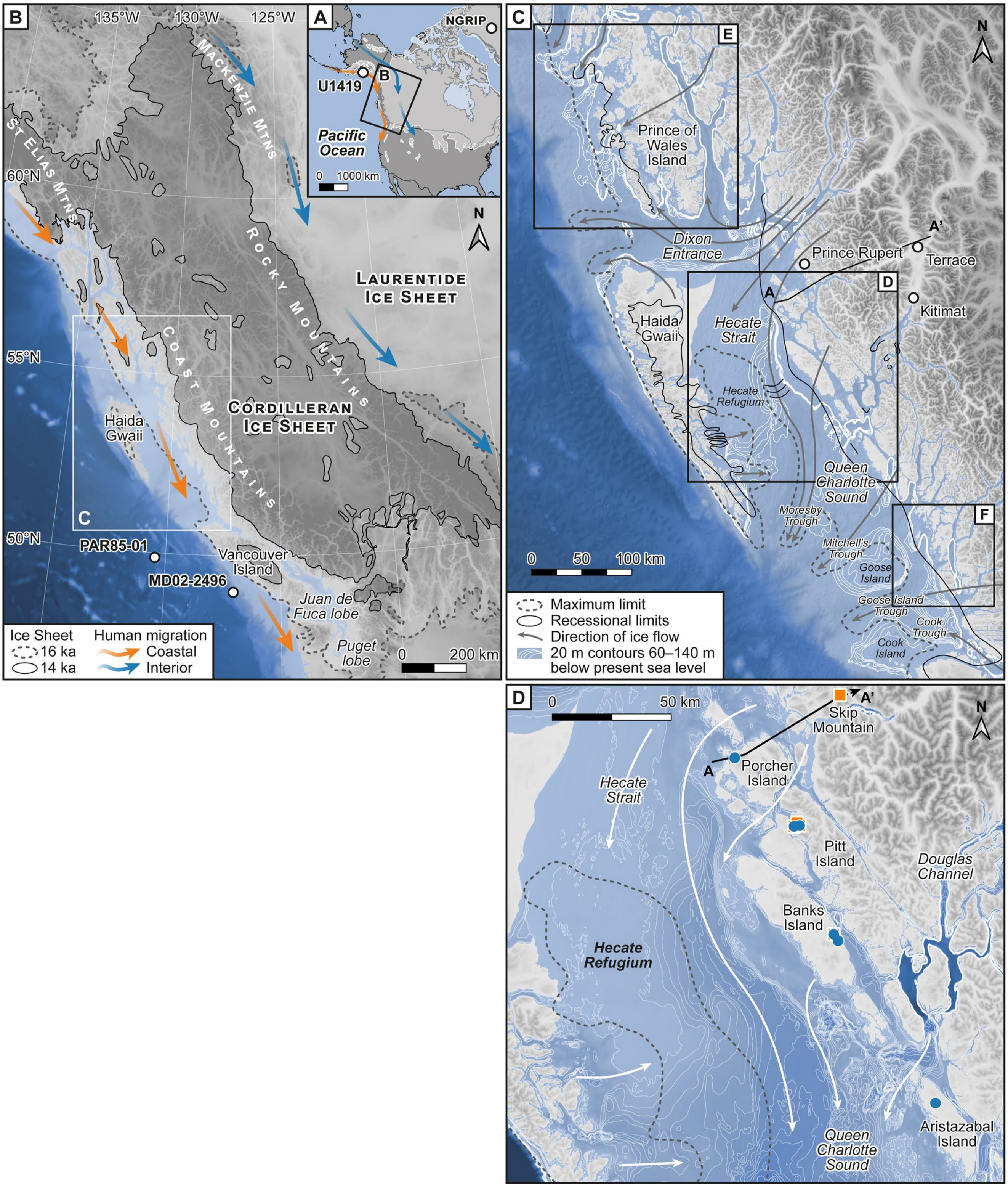

B
135°W
130°W
125°W
MACKENZIE MTNS
ST ELIAS MTNS
ROCKY MOUNTAINS
COAST MOUNTAINS
60°N
55°N
50°N
LAURENTIDE ICE SHEET
CORDILLERAN ICE SHEET
Haida Gwaii
C
PAR85-01
MD02-2496
Vancouver Island
Juan de Fuca lobe
Puget lobe
0
200 km
Ice Sheet
16 ka
14 ka
Human migration
Coastal
Interior
A
NGRIP
U1419
B
Pacific Ocean
0
1000 km
C
E
Prince of Wales Island
Dixon Entrance
Prince Rupert
A'
Terrace
D
A
Kitimat
Haida Gwaii
Hecate Strait
Hecate Refugium
Queen Charlotte Sound
Moresby Trough
Mitchell's Trough
Goose Island
F
Goose Island Trough
Cook Trough
Cook Island
0
50
100 km
Maximum limit
Recessional limits
Direction of ice flow
20 m contours 60–140 m below present sea level
D
0
50 km
A'
Skip Mountain
A
Porcher Island
Hecate Strait
Pitt Island
Douglas Channel
Banks Island
Hecate Refugium
Queen Charlotte Sound
Aristazabal Island

Figure 1.

resolve the drivers of ice retreat during the onset of deglaciation (Darvill et al., 2018; Lesnek et al., 2018; Shaw et al., 2020). This study targets islands on the central coast of British Columbia, Canada, to establish the synchroneity of deglaciation on the western Cordilleran Ice Sheet margin. We aim to reconstruct the timing of ice retreat to understand ice sheet geometry through time, with implications for ice-climate interactions, sea level rise and ice-free islands along a coastal human migration route.

2. Study Area

Our study area focuses on four islands on the central coast of British Columbia, from north to south: Porcher (53.97°N, 130.60°W), Pitt (53.73°N, 130.19°W), Banks (53.32°N, 129.88°W), and Aristazabal (52.72°N, 129.21°W; Figure 1d). Collectively, the islands span ∼200 km north-south along the present-day coastline, linking the study areas of Lesnek et al. (2018, 2020) and Darvill et al. (2018) across ∼600 km, and should record ice retreat from Haida Gwaii, across Hecate Strait and into the Coast Mountains (Blaise et al., 1990; Clague et al., 1982; Mathewes & Clague, 2017; Shaw et al., 2020; Warner et al., 1982). The abundance of quartz-bearing erratic boulders and glacially smoothed bedrock in the study area is ideal for surface exposure dating using ^{10}Be nuclides (Cui et al., 2017). Subaerial glacial landforms are relatively sparse, but Shaw et al. (2020) provide a detailed framework from bathymetric data upon which to develop a glacial geochronology.

At its last maximum, the Cordilleran Ice Sheet flowed across the Coast Mountains to the continental shelf, north through Dixon Entrance, south through Hecate Strait, and coalescing with local ice on Haida Gwaii (Eyles et al., 2018; Josenhans, 1994; Josenhans et al., 1995; Seguinot et al., 2016; Shaw et al., 2020), but leaving the "Hecate Refugium" ice-free (Figure 1c; Mathewes & Clague, 2017). Ice in Queen Charlotte Sound, south of Hecate Strait, formed an extensive, 200–300 km margin (Barrie & Conway, 1999, 2002a; Blaise et al., 1990; Luternauer et al., 1989; Margold et al., 2013), grounded and topographically constrained within troughs (Shaw et al., 2020). Ice-rafted debris has been linked to calving along the west coast (Blaise et al., 1990; Hendy & Cosma, 2008; Taylor et al., 2014) although Moresby Trough may have hosted the only ice shelf in the study area at the last glacial maximum (Shaw et al., 2020). Inland sites track late stages of deglaciation into fjords (Clague, 1985) as ice retreated and thinned into the Coast Mountains (Menounos et al., 2017).

The timing of retreat for the central western ice margin remains poorly constrained. In particular, a chronological gap around Prince Rupert (Figure 1d) makes it challenging to link marginal positions between Vancouver Island (Al-Suwaidi et al., 2006) and Calvert Island (Darvill et al., 2018) to the South (Figure 1f), Haida Gwaii to the west (Mathewes & Clague, 2017), Prince of Wales Island to the north (Figure 1e; Lesnek et al., 2018, 2020), and Terrace to the east (Clague, 1985). It is also unclear how the western ice sheet margin responded to thinning in the interior at 14.5–12.5 ka (Menounos et al., 2017).

3. Methods

We determined ages from erratic boulders (n = 15) and bedrock surfaces (n = 5) exposed by retreating ice to reconstruct the timing of deglaciation from the four islands in our study area (Figure 1d and Table S1; sample context in the Supporting Information S1). We sampled topmost surfaces of erratic boulders and glacially smoothed bedrock with an angle grinder and/or hammer and chisel. Locations and altitudes were measured using a handheld GPS (estimated ±5 m) and we recorded topographic shielding and strike/dip of boulder and bedrock samples with a compass-clinometer. We collected samples from two sites spanning >300 m elevation. Samples from Pitt Island are between 884 and 333 m above sea level (a.s.l.) within ∼2.4 km, forming a vertical transect of erratic boulders and glacially smoothed bedrock past which the ice sheet flowed. On Banks Island,

Figure 1. (a) Location and (b) approximate extent of the Cordilleran Ice Sheet at 16 ka (dashed black lines) and 14 ka (solid black lines) (Dyke, 2004). Arrows show possible routes proposed for early human migration through the Americas: one coastal (orange) along the present coastline of Alaska and British Columbia; the other interior (blue) between the Cordilleran and Laurentide Ice Sheets. Locations of the NGRIP ice core and U-1419, PAR85-01, and MD02-2496 marine cores in Figure 4 are shown. (c) The western coast of North America showing the study areas of (d) this study; (e) Lesnek et al. (2018, 2020); and (f) Darvill et al. (2018). Hypothesized maximum (dashed gray lines) and recessional ice limits (solid gray lines) as well as ice flow lines (gray arrows) are from Shaw et al. (2020) and Lesnek et al. (2018). White lines are 20 m contours 60–140 m below present sea level to highlight bathymetric topography and palaeoislands, although relative sea level history is complex (see main text). Transect A–A' in Figure 3 is shown. (d) Study area in detail, including sampling sites: blue circles are erratic boulders; orange squares are glacially smoothed bedrock. Detailed sample information and context is in Table S1 and Figures S5–S9 in Supporting Information S1. White lines are 20 m contour lines 0–400 m below sea level.

samples were collected between 425 and 78 m a.s.l. within ∼3.3 km of one another (Figures S5–S9 in Supporting Information S1).

The Tulane University Cosmogenic Nuclide Laboratory performed physical and chemical preparations, and Purdue University Rare Isotope Laboratory measured $^{10}Be/^{9}Be$ isotope ratios. We used Version 3 of Balco et al.'s (2008) online calculator (http://hess.ess.washington.edu/) to calculate ^{10}Be exposure ages relative to the production rate data set in Borchers et al. (2016) and "LSDn" scaling scheme (Lifton et al., 2014). None of the ages were corrected for surface erosion, snow cover or glacioisostatic adjustment, so represent minimum exposure ages for ice retreat. Relative sea level in this region is complex and relatively unknown prior to around 15.0 ka (Letham et al., 2016, 2021; Shugar et al., 2014), but a hypothesized "hinge" of stability along the present coastal margin implies some islands experienced little sea level change during deglaciation (Fedje et al., 2018; Hetherington et al., 2004; McLaren et al., 2014; Shugar et al., 2014).

We present and discuss exposure ages with internal, analytical errors and as groups from each site using interquartile ranges (IQR) to provide a conservative estimate of age uncertainty in light of possible postdepositional snow cover, erosion, or exhumation (Menounos et al., 2017). We present ranges without excluding outliers to better account for possible geomorphic uncertainty—arguably the largest source of error in exposure dating (Balco, 2020). IQR and median ages yield similar results to weighted means and standard errors calculated to include uncertainty on the production rate (Table S1 and Figures S1–S4 in Supporting Information S1). We show in the Supporting Information that removing potential outliers or using the weighted mean age for each study site does not alter our findings.

For consistency, we recalculated published exposure ages using the methods above (Table S1). These samples, collected during 2015–2017, are denoted by sample ID prefixes (Darvill et al., 2018; Lesnek et al., 2018, 2020) and differ slightly from those originally published without affecting original conclusions.

4. Results

Erratic boulders and glacially smoothed bedrock on Banks Island yield ^{10}Be exposure ages from 18.8 ± 0.7 to 13.6 ± 0.6 ka ($n = 6$, IQR = 17.7–16.3 ka; Figure 2). On Aristazabal Island, erratic boulders provided exposure ages of 16.1 ± 0.6 to 14.3 ± 0.6 ka ($n = 3$, IQR = 16.0–15.1 ka). Erratic boulders and glacially smoothed bedrock on Pitt Island yield exposure ages of 18.7 ± 0.9 to 12.7 ± 1.1 ka ($n = 6$, IQR = 17.2–13.8 ka). On Porcher Island, erratic boulders returned exposure ages of 18.8 ± 0.9 to 11.8 ± 0.5 ka ($n = 4$, IQR = 15.6–12.8 ka). At higher elevation, glacially smoothed bedrock from Skip Mountain, at 1,067 m a.s.l., provided an exposure age of 15.1 ± 1.1 ka.

Two samples from Banks Island are from surfaces 300 m above the others. Samples from above 400 m a.s.l. range from 17.1 ± 0.5 to 16.0 ± 0.6 ka ($n = 2$) and samples below 100 m a.s.l. range from 18.8 ± 0.7 to 13.6 ± 0.6 ka ($n = 4$). The high and low elevation groups are in reverse stratigraphic order but overlap within errors. We cannot rule out that all samples record a complex ice marginal position, with the ice sheet terminus abutting higher and lower elevations (Figure S6 in Supporting Information S1). Consequently, it is not clear at this site whether elevation difference relates to thinning or the ice sheet terminating against an area of higher land.

On Pitt Island, two samples are from 880 to 884 m a.s.l., yielding ages of 15.1 ± 0.5 and 13.6 ± 0.8 ka. A sample at 589 m a.s.l. yielded an age of 17.9 ± 2.2 ka and three samples from 333 to 342 m a.s.l. ranged from 18.7 ± 0.9 to 12.7 ± 1.1 ka. We are more confident that samples from Pitt Island represent a true vertical transect, with ice flowing past and thinning through time, supported by exposure ages from Porcher Island of ca. 15.6–12.8 ka (Figures 3a and 3b). Hence, we observe a reduction in ice sheet elevation of ∼545 m between high (IQR = 14.7–14.0 ka) and low elevation sites (IQR = 16.4–13.4). However, we caution that we cannot rule out nonlinear thinning or thinning during concurrent lateral retreat from the data available.

5. Discussion

5.1. Ice Retreat on the Central Coast

Our ^{10}Be exposure ages show ice on the central coast of British Columbia reached Banks Island by at least 17.7–16.3 ka, Aristazabal Island by 16.0–15.1 ka, Pitt Island by 17.2–13.8 ka and Porcher island 15.6–12.8 ka,

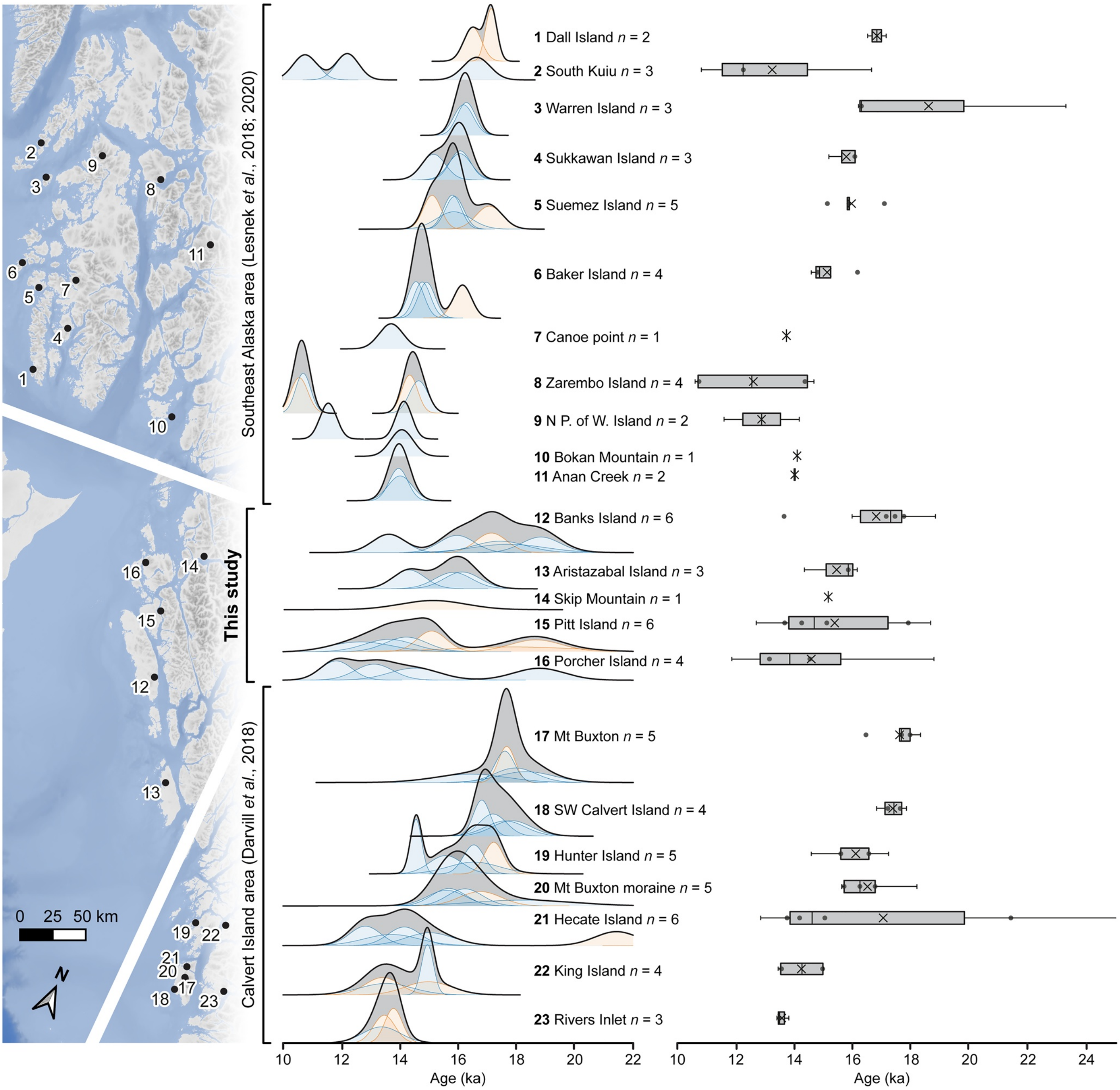

Figure 2. Density function plots for individual ages from three study areas (boulders in blue, bedrock in orange) and cumulatively for each study site (black lines and gray shading). Box and whisker plots summarize all ages at each site, including the median (black vertical line), mean (black cross) and IQR (25–75%; gray box widths). Study sites are arranged oldest to youngest across each study area, named and numbered according to the overview map, with the number of samples (n) at each site.

respectively (Figures 2 and 3c–3f). We find a consistent pattern in the timing of exposure by ice along the west coast of North America (Figures 2 and 3; Darvill et al., 2018; Lesnek et al., 2018, 2020). This chronology accords with other constraints showing the Cordilleran Ice Sheet advanced across Hecate Strait to coalesce with local ice on Haida Gwaii after ca. 30.0 ka, reaching the continental shelf margin before retreating from Haida Gwaii toward the mainland by ca. 19.4 ka (Figure 3d; Blaise et al., 1990; Clague et al., 1982; Margold et al., 2013; Mathewes & Clague, 2017; Taylor et al., 2014; Warner et al., 1982). Radiocarbon ages from Prince of Wales Island to the north suggest ice may have advanced slightly later, between ca. 19.8 and

10.1029/2021GL097191

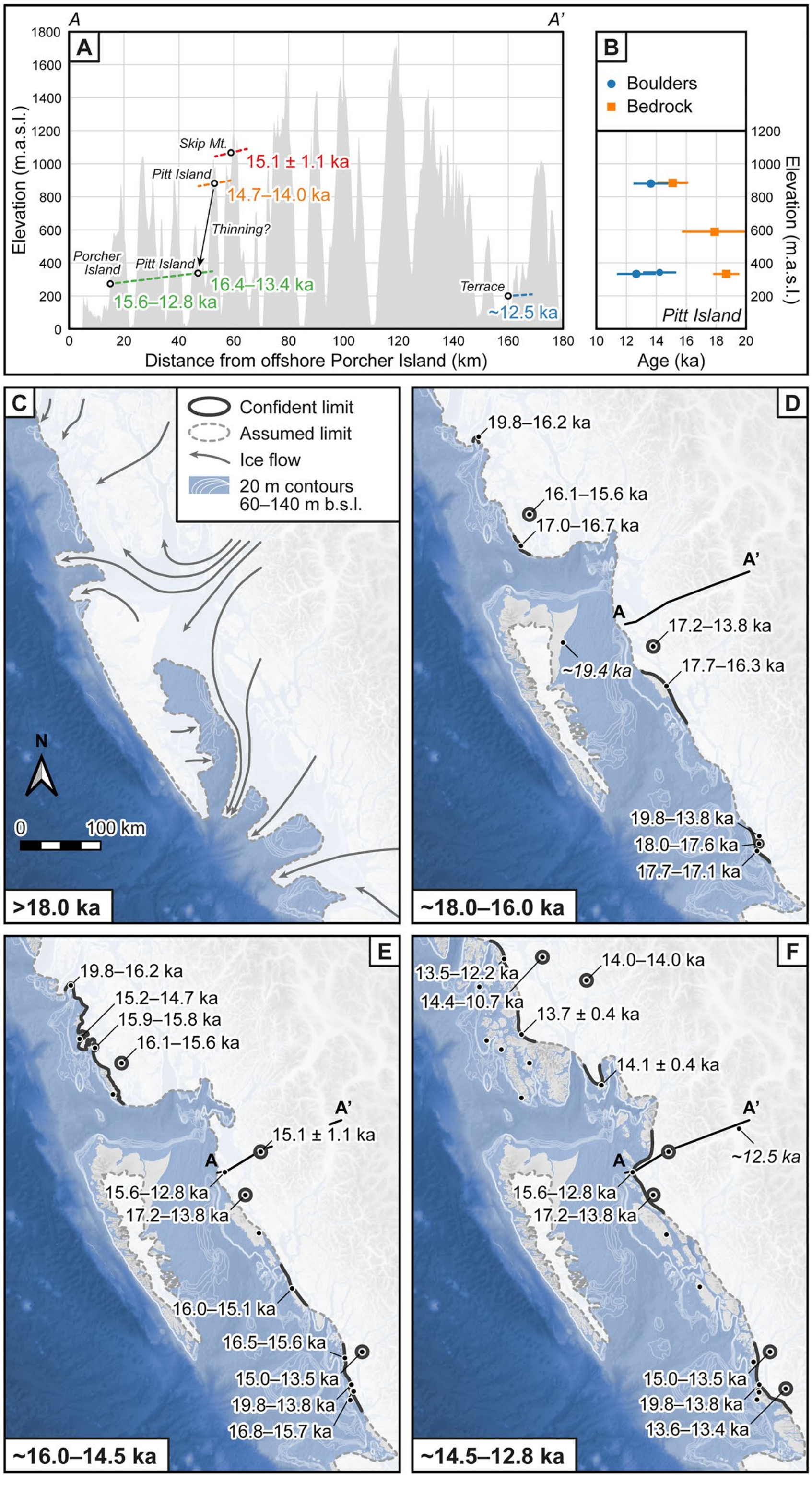

Figure 3. (a) Schematic transect through the Coast Mountains highlighting the difference in ice sheet elevation through the last deglaciation (A–A' in D–F and Figures 1c and 1d). Pitt and Porcher Islands are interquartile ranges; Terrace radiocarbon age is from Clague et al. (1985). (b) Exposure ages from Pitt Island against elevation. Blue circles are from erratic boulders, orange squares are from bedrock. (c–f) Four time-steps based on our exposure age chronology illustrating the broad timing of coastal deglaciation. Some sites were exposed prior to lateral retreat and are assumed to show higher-altitude thinning at the same time as marginal retreat (circles within the main body of the ice sheet). Ages are IQRs except for single-sample sites (exposure ages and internal errors. Italic ages in (d, f) are minimum radiocarbon ages for ice retreat of 19.4 ka (Mathewes & Clague, 2017) and 12.5 ka (Clague, 1985).

17.2 ka (Lesnek et al., 2018). Radiocarbon ages from Vancouver Island to the south limit ice advance to between ca. 19.6 and ca. 15.7 ka (Al-Suwaidi et al., 2006), consistent with either scenario. Overall, there is a coherent pattern of ice advancing between ca. 30.0 and 17.7 ka and retreating back to the present coastline by around 18–16 ka.

Retreat slowed once ice reached the present coastline. Numerous sites along the coastline were exposed between ca. 18.0–12.8 ka (Figures 3d–3f and 4i), suggesting the western ice sheet margin retreated by less than 100 km (and generally <50 km) for around 4–5 kyr (Figure 3). It is possible ice readvanced to approximately the same position on multiple occasions, but we cannot resolve readvances from the available data. A radiocarbon age of 14.4–14.1 ka from marine shell fragments at Prince Rupert (Lowdon & Blake, 1979) is consistent with the deglaciation of nearby Pitt Island and Porcher Island by at least 13.8–12.8 ka. Radiocarbon-dated sea level records indicate the central Douglas Channel was ice-free by 14.5 ka (Letham et al., 2021) and Prince Rupert was ice-free by 15.0–14.5 ka (Letham et al., 2016). Slightly older radiocarbon ages are not necessarily at odds with our chronology given the exposure ages are minima for deglaciation. Additionally, the ice margin was likely complex, such that fjords and inlets could have become ice-free before final deglaciation of island pinning points to allow ice retreat through the Kitimat Trough to reach Terrace by 12.6–12.1 ka (Figures 3e and 3f; Clague, 1985). The fact the Cordilleran Ice Sheet remained extensive, close to the present coast, throughout deglaciation agrees with radiocarbon chronologies for glaciation and sea level change along the coastline (Eamer et al., 2017; Letham et al., 2016, 2021; Margold et al., 2014) but differs from records on the southern ice margin (Porter & Swanson, 1998) and is not well captured by ice sheet models (Seguinot et al., 2014, 2016). Hence, we find an ice sheet sector can achieve prolonged lateral stability during deglaciation.

Exposure ages from Pitt Island hint at thinning during the period of ice margin stabilization. Approximately 500 m of vertical ice may have been lost from Pitt Island between ca. 17.2–13.8 ka (Figure 3b), consistent with deglaciation of the top of nearby Skip Mountain (1,067 m.a.s.l.) by 15.1 ka and of the deglaciation of low-altitude Porcher Island to the west by 15.6–12.8 ka (Figure 3a). We cannot refine thinning rates from the data available, but the timing is consistent with that hypothesized (Margold et al., 2014) and quantified (Menounos et al., 2017) for the ice sheet interior from around 14.0 ka. Further work should test whether pan-ice sheet mass loss occurred during deglaciation. From the evidence available, it appears ice mass may be lost through thinning without substantial marginal retreat, highlighting the importance of examining both vertical and lateral change.

Our findings demonstrate ice reached the present coast along much of western North America before a phase of human migration at 14.7–12.9 ka (Figure 1b; Becerra-Valdivia & Higham, 2020; Waters, 2019). Dixon Entrance, Hecate Strait and Queen Charlotte Sound were all ice-free, as well as numerous islands including the hypothesized "Hecate Refugium" (Mathewes & Clague, 2017; Shaw et al., 2020), palaeo-Goose and palaeo-Cook Islands (Barrie & Conway, 2002b; Luternauer et al., 1989), and northern Vancouver Island (Hebda et al., 2022). Our exposure ages reveal ice remained along the present coastline for several thousand years, so migration along the coastal route would have been between islands only tens of kilometers from an ice sheet margin.

5.2. Drivers of Change

The onset of retreat of the western Cordilleran Ice Sheet from its maximum at the continental shelf began prior to around 18.0 ka (this study; Darvill et al., 2018) and perhaps slightly later in southeast Alaska (Lesnek et al., 2018, 2020). Initial deglaciation occurred during rising insolation at 60°N (Berger & Loutre, 1991), but atmospheric temperatures in the Northern Hemisphere (Andersen et al., 2004) and local surface ocean temperatures in the eastern Pacific (Taylor et al., 2014) remained relatively cool (Figures 4a–4d). Average regional ocean surface temperatures suggest an anomalously warm Northeast Pacific at ~18 ka (Figure 4e; Praetorius et al., 2020), clearer in alkenone-based reconstructions than Mg/Ca records. Eustatic sea level had also risen by ~10 m by 18 ka (Figure 4h; Lambeck et al., 2014). Hence, destabilization of marine-terminating parts of the ice sheet may have been triggered by sea level rise and/or regional ocean warming.

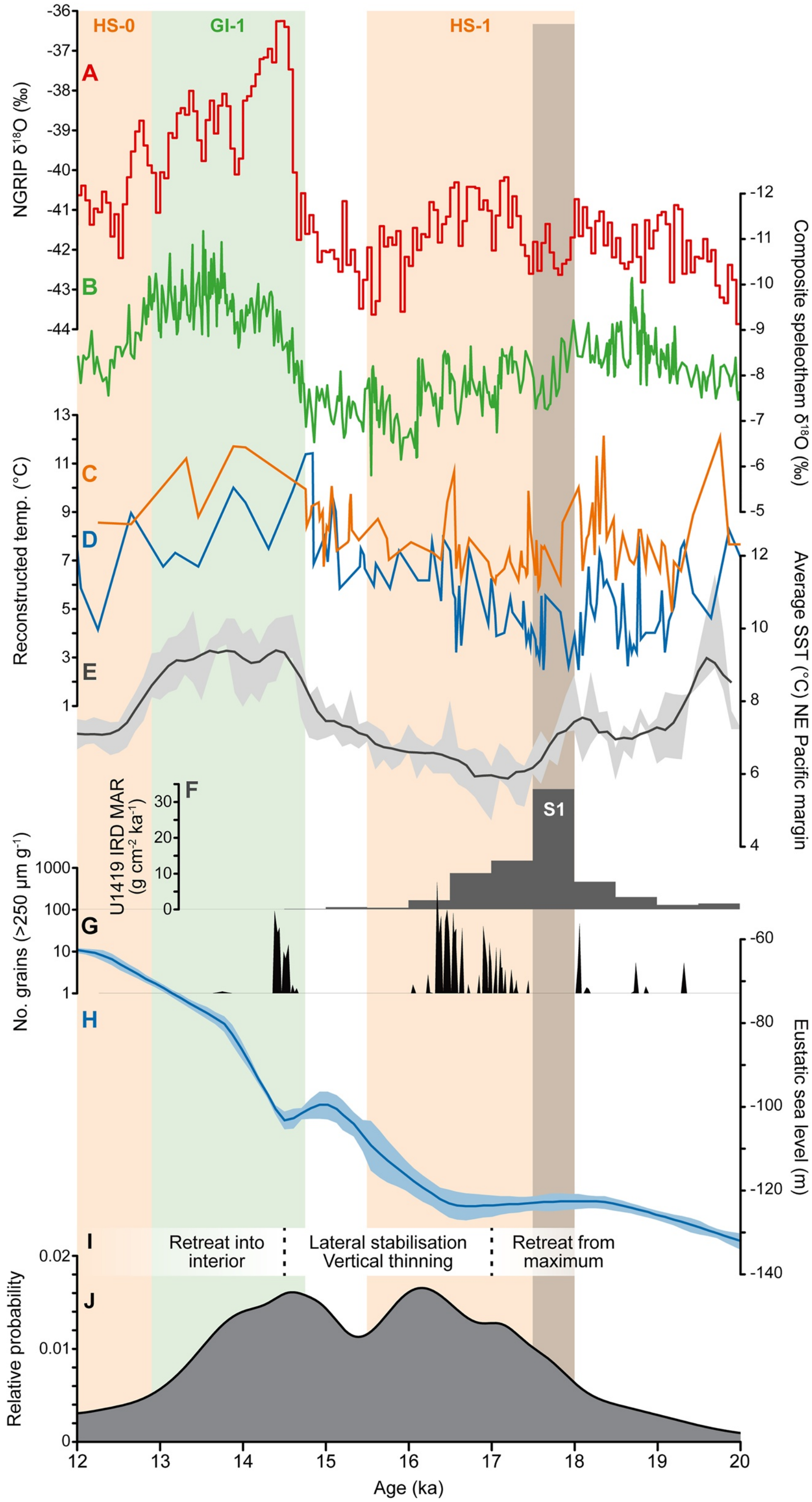
HS-0
GI-1
HS-1
S1
A
B
C
D
E
F
G
H
I
J
NGRIP δ18O (‰)
Composite speleothem δ18O (‰)
Reconstructed temp. (°C)
Average SST (°C) NE Pacific margin
U1419 IRD MAR (g cm-2 ka-1)
No. grains (>250 μm g-1)
Eustatic sea level (m)
Retreat into interior
Lateral stabilisation Vertical thinning
Retreat from maximum
Relative probability
Age (ka)

Figure 4.

10.1029/2021GL097191

North Pacific warming has been linked to a relatively strong Asian monsoon system between ~20 and 18 ka (Figure 4b) and initiation or exacerbation of marine-based ice retreat in the Gulf of Alaska (Walczak et al., 2020). Our record of ice retreat accords with the youngest peak in ice-rafted debris in the Gulf of Alaska U1419 marine core (Siku Event S1; Figure 4f; Walczak et al., 2020). This raises the possibility that marine-terminating ice margin collapse in our study area contributed toward Siku events in the North Pacific, with ice-rafted debris transported by the northward-flowing Alaska Current toward the Gulf of Alaska. Resolving whether initial destabilization was driven by rising sea level or incursions of warmer ocean currents around marine-terminating margins requires better-resolved records of local sea level and ocean temperature change for 18.0–15.0 ka.

During destabilization, ice sheet discharge may have been enhanced by ice streaming through Dixon Entrance and Hecate Strait (Eyles et al., 2018; Shaw et al., 2020). In Hecate Strait, ice retreated ~100 km from Haida Gwaii to the present coast within ~2 ka. This is slower than modeled ice stream grounding line retreat (Gandy et al., 2018), but moraines preserved on the seafloor suggest retreat could have been stepwise (Shaw et al., 2017, 2020). Punctuated retreat may explain small spikes in ice-rafted debris off Vancouver Island (MD02-2496) prior to 18.0 ka (Figure 4g; Hendy & Cosma, 2008; Taylor et al., 2014), possibly linked to an ice shelf in Moresby Trough (Shaw et al., 2020).

The western margin of the Cordilleran Ice Sheet apparently stabilized once it reached the present-day coastline, after ca. 18 ka (Figures 3 and 4i–4j). Northern Hemisphere temperatures remained cool (Figure 4a; Andersen et al., 2004), as did local ocean temperatures (Figures 4c and 4d; Taylor et al., 2014). With conditions seemingly unfavorable for strong mass loss, the topography of the present coastline could have presented a stable pinning position for the ice sheet over the next 4–5 kyr. This stabilization was despite warming atmospheric and ocean temperatures during Greenland Interstadial-1 (the Bølling-Allerød period) and rapid eustatic sea level rise (Figures 4a–4h; Andersen et al., 2004; Lambeck et al., 2014; Praetorius et al., 2020; Taylor et al., 2014). Potential ice sheet thinning could have resulted in relative sea level fall, further enhancing stability. Coastal islands may have allowed a transition toward a land-terminating western ice margin, with smaller, more stable marine-terminating outlets situated within present-day fjords, similar to ice retreat on the west coast of Scandinavia (Briner et al., 2014; Mangerud et al., 2016; Svendsen et al., 2015).

6. Conclusions

Our study shows at least ~600 km of the western Cordilleran Ice Sheet margin had retreated to the present coastline by ca. 18–16 ka. Ice most likely retreated from Hecate Strait, Queen Charlotte Sound and Dixon Entrance in the early stages of deglaciation due to destabilization of marine-terminating margins enhanced by eustatic sea level rise and/or ocean warming. Once ice reached the present coast, its margin became relatively stable for ~4–5 kyr, or consistently readvanced to the same position. During this time, the ice sheet may have thinned markedly in its interior—and perhaps to its western edge—by ca. 13 ka. Our new reconstruction demonstrates an ice sheet sector can reach prolonged lateral stability during overall retreat. However, mass may still be lost through thinning without substantial marginal retreat, with implications for reconstructing and modeling past and future ice sheet change and meltwater contribution to sea level rise. Additional studies should employ vertical chronological transects to better quantify the timing and rate of volumetric change of the Cordilleran Ice Sheet. The timing of ice retreat from our chronology also shows that several hundred kilometers of the coastline were ice-free prior to a significant phase of early human migration through the continent.

Figure 4. Synthesis of selected proxy records and the timing of Cordilleran Ice Sheet deglaciation. Timing is shown for Heinrich Stadials (orange bars) HS-1 and HS-0 (the Younger Dryas period), Greenland Interstadial (green bar) GI-1 (the Bølling-Allerød period), and Siku Event S1 (brown bar). (a) North Greenland Ice Core Project (NGRIP) $\delta^{18}O$ (location in Figure 1a) (Andersen et al., 2004); (b) Composite speleothem $\delta^{18}O$ as a proxy for Asian Monsoon strength (Cheng et al., 2016) (c) Reconstructed Mg/Ca temperatures for *N. pachyderma* and (d) *G. bulloides* from marine core MD02-2496 (location in Figure 1b) (Taylor et al., 2014); (e) Average Sea Surface Temperature (SST) of Northeast (NE) Pacific margin sites (Praetorius et al., 2020); (f) Ice-rafted debris record from core U1419 (location in Figure 1a) (Walczak et al., 2020); (g) Ice-rafted debris record on a logarithmic scale from core MD02-2496 (Taylor et al., 2014); (h) Ice volume equivalent, eustatic sea level (Lambeck et al., 2014); (i) Pattern of Cordilleran Ice Sheet retreat from Figure 3; (j) Summed probability of all exposure ages in Figure 2 to highlight broad timing of ice retreat.

Data Availability Statement

All data available in supporting information at https://doi.org/10.48420/15147366.

Acknowledgments

This research was funded by National Geographic Society Grant CP-115R-17 with additional support from The University of Manchester SEED Strategic Early Career Fund. We thank PRIME Lab staff for beryllium isotope ratio measurements. Menounos acknowledges funding from the National Science and Engineering Research Council of Canada and the Canada Research Chairs Program. This paper has benefitted from the comments of Bethan Davies, three anonymous reviewers and the editor Mathieu Morlighem.

References

Al-Suwaidi, M., Ward, B. C., Wilson, M. C., Hebda, R. J., Nagorsen, D. W., Marshall, D., et al. (2006). Late Wisconsinan Port Eliza cave deposits and their implications for human coastal migration, Vancouver island, Canada. *Geoarchaeology*, *21*(4), 307–332. https://doi.org/10.1002/gea.20106

Andersen, K. K., Azuma, N., Barnola, J.-M., Bigler, M., Biscaye, P., Caillon, N., et al. (2004). High-resolution record of Northern Hemisphere climate extending into the last interglacial period. *Nature*, *431*(7005), 147–151. https://doi.org/10.1038/nature02805

Balco, G. (2020). Glacier change and paleoclimate applications of cosmogenic-nuclide exposure dating. *Annual Review of Earth and Planetary Sciences*, *48*, 21–48. https://doi.org/10.1146/annurev-earth-081619-052609

Balco, G., Stone, J. O., Lifton, N. A., & Dunai, T. J. (2008). A complete and easily accessible means of calculating surface exposure ages or erosion rates from 10Be and 26Al measurements. *Quaternary Geochronology*, *3*(3), 174–195. https://doi.org/10.1016/j.quageo.2007.12.001

Barrie, J. V., & Conway, K. W. (1999). Late quaternary glaciation and postglacial stratigraphy of the northern Pacific margin of Canada. *Quaternary Research*, *51*(2), 113–123. https://doi.org/10.1006/qres.1998.2021

Barrie, J. V., & Conway, K. W. (2002a). Contrasting glacial sedimentation processes and sea-level changes in two adjacent basins on the Pacific margin of Canada. *Geological Society, London, Special Publications*, *203*(1), 181–194. https://doi.org/10.1144/gsl.sp.2002.203.01.10

Barrie, J. V., & Conway, K. W. (2002b). Rapid sea-level change and coastal evolution on the Pacific margin of Canada. *Sedimentary Geology*, *150*(1), 171–183. https://doi.org/10.1016/s0037-0738(01)00274-3

Becerra-Valdivia, L., & Higham, T. (2020). The timing and effect of the earliest human arrivals in North America. *Nature*, *584*(7819), 93–97. https://doi.org/10.1038/s41586-020-2491-6

Bennett, M. R., Bustos, D., Pigati, J. S., Springer, K. B., Urban, T. M., Holliday, V. T., et al. (2021). Evidence of humans in North America during the Last Glacial Maximum. *Science*, *373*(6562), 1528–1531. https://doi.org/10.1126/science.abg7586

Berger, A., & Loutre, M. F. (1991). Insolation values for the climate of the last 10 million years. *Quaternary Science Reviews*, *10*(4), 297–317. https://doi.org/10.1016/0277-3791(91)90033-q

Blaise, B., Clague, J. J., & Mathewes, R. W. (1990). Time of maximum late Wisconsin glaciation, west coast of Canada. *Quaternary Research*, *34*(1), 282–295. https://doi.org/10.1016/0033-5894(90)90041-i

Borchers, B., Marrero, S., Balco, G., Caffee, M., Goehring, B., Lifton, N., et al. (2016). Geological calibration of spallation production rates in the CRONUS-Earth project. *Quaternary Geochronology*, *31*, 188–198. https://doi.org/10.1016/j.quageo.2015.01.009

Briner, J. P., Svendsen, J. I., Mangerud, J., Lohne, Ø. S., & Young, N. E. (2014). A ^{10}Be chronology of south-Western Scandinavian Ice Sheet history during the Lateglacial period. *Journal of Quaternary Science*, *29*(4), 370–380. https://doi.org/10.1002/jqs.2710

Cheng, H., Edwards, R. L., Sinha, A., Spötl, C., Yi, L., Chen, S., et al. (2016). The Asian monsoon over the past 640,000 years and ice age terminations. *Nature*, *534*(7609), 640–646. https://doi.org/10.1038/nature18591

Clague, J. J. (1985). Deglaciation of the Prince Rupert—Kitimat area, British Columbia. *Canadian Journal of Earth Sciences*, *22*(2), 256–265. https://doi.org/10.1139/e85-022

Clague, J. J., Mathewes, R. W., & Warner, B. G. (1982). Late Quaternary geology of eastern Graham island, Queen Charlotte islands, British Columbia. *Canadian Journal of Earth Sciences*, *19*(9), 1786–1795. https://doi.org/10.1139/e82-157

Clark, J., Carlson, A. E., Reyes, A. V., Carlson, C. B., Guillaume, L., Milne, G. A., et al. (2022). The age of the opening of the Ice-Free Corridor and implications for the peopling of the Americas. *Proceedings of the National Academy of Sciences*, *119*(14), e2118558119. https://doi.org/10.1073/pnas.2118558119

Cui, Y., Miller, D., Schiarizza, P., & Diakow, L. J. (2017). British Columbia digital geology. In *British Columbia geological survey open file (Mines Petrol. Resour. No. 2017-8, 9 p.)*. British Columbia Ministry of Energy.

Darvill, C. M., Menounos, B., Goehring, B. M., Lian, O. B., & Caffee, M. W. (2018). Retreat of the Western Cordilleran ice sheet margin during the last deglaciation. *Geophysical Research Letters*, *45*(18), 9710–9720. https://doi.org/10.1029/2018GL079419

Dyke, A. S. (2004). An outline of North American deglaciation with emphasis on central and northern Canada. In *Developments in Quaternary Sciences* (Vol. 2, pp. 373–424). Elsevier. https://doi.org/10.1016/s1571-0866(04)80209-4

Eamer, J. B. R., Shugar, D. H., Walker, I. J., Lian, O. B., Neudorf, C. M., & Telka, A. M. (2017). A glacial readvance during retreat of the Cordilleran Ice Sheet, British Columbia central coast. *Quaternary Research*, *87*(3), 468–481. https://doi.org/10.1017/qua.2017.16

Eyles, N., Arbelaez Moreno, L., & Sookhan, S. (2018). Ice streams of the late Wisconsin Cordilleran ice sheet in Western North America. *Quaternary Science Reviews*, *179*, 87–122. https://doi.org/10.1016/j.quascirev.2017.10.027

Fedje, D., McLaren, D., James, T. S., Mackie, Q., Smith, N. F., Southon, J. R., & Mackie, A. P. (2018). A revised sea level history for the northern Strait of Georgia, British Columbia, Canada. *Quaternary Science Reviews*, *192*, 300–316. https://doi.org/10.1016/j.quascirev.2018.05.018

Froese, D., Young, J. M., Norris, S. L., & Margold, M. (2019). Availability and viability of the Ice-Free corridor and Pacific Coast routes for the peopling of the Americas. *SAA Archaeological Record*, *19*, 27–33.

Gandy, N., Gregoire, L. J., Ely, J. C., Clark, C. D., Hodgson, D. M., Lee, V., et al. (2018). Marine ice sheet instability and ice shelf buttressing of the Minch Ice Stream, northwest Scotland. *The Cryosphere*, *12*(11), 3635–3651. https://doi.org/10.5194/tc-12-3635-2018

Gomez, N., Gregoire, L. J., Mitrovica, J. X., & Payne, A. J. (2015). Laurentide-Cordilleran Ice Sheet saddle collapse as a contribution to meltwater pulse 1A. *Geophysical Research Letters*, *42*, 3954–3962. https://doi.org/10.1002/2015GL063960

Gregoire, L. J., Otto-Bliesner, B., Valdes, P. J., & Ivanovic, R. (2016). Abrupt Bølling warming and ice saddle collapse contributions to the Meltwater Pulse 1a rapid sea level rise. *Geophysical Research Letters*, *43*, 9130–9137. https://doi.org/10.1002/2016GL070356

Gregoire, L. J., Payne, A. J., & Valdes, P. J. (2012). Deglacial rapid sea level rises caused by ice-sheet saddle collapses. *Nature*, *487*(7406), 219–222. https://doi.org/10.1038/nature11257

Hebda, C. F. G., McLaren, D., Mackie, Q., Fedje, D., Pedersen, M. W., Willerslev, E., et al. (2022). Late Pleistocene palaeoenvironments and a possible glacial refugium on northern Vancouver Island, Canada: Evidence for the viability of early human settlement on the northwest coast of North America. *Quaternary Science Reviews*, *279*, 107388. https://doi.org/10.1016/j.quascirev.2022.107388

Hendy, I. L., & Cosma, T. (2008). Vulnerability of the Cordilleran Ice Sheet to iceberg calving during late Quaternary rapid climate change events. *Paleoceanography*, *23*, PA2101. https://doi.org/10.1029/2008PA001606

Hetherington, R., Barrie, J. V., Reid, R. G. B., MacLeod, R., & Smith, D. J. (2004). Paleogeography, glacially induced crustal displacement, and Late Quaternary coastlines on the continental shelf of British Columbia, Canada. *Quaternary Science Reviews*, *23*(3), 295–318. https://doi.org/10.1016/j.quascirev.2003.04.001

Josenhans, H. W. (1994). *Surficial geology, quaternary stratigraphy and paleoenvironments of Queen Charlotte basin*. Geological Survey of Canada.

Josenhans, H. W., Fedje, D. W., Conway, K. W., & Barrie, J. V. (1995). Post glacial sea levels on the Western Canadian continental shelf: Evidence for rapid change, extensive subaerial exposure, and early human habitation. *Marine Geology*, *125*(1–2), 73–94. https://doi.org/10.1016/0025-3227(95)00024-s

Lambeck, K., Rouby, H., Purcell, A., Sun, Y., & Sambridge, M. (2014). Sea level and global ice volumes from the Last Glacial Maximum to the Holocene. *Proceedings of the National Academy of Sciences of the United States of America*, *111*(43), 15296–15303. https://doi.org/10.1073/pnas.1411762111

Lesnek, A. J., Briner, J. P., Baichtal, J. F., & Lyles, A. S. (2020). New constraints on the last deglaciation of the Cordilleran Ice Sheet in coastal southeast Alaska. *Quaternary Research*, *96*, 140–160. https://doi.org/10.1017/qua.2020.32

Lesnek, A. J., Briner, J. P., Lindqvist, C., Baichtal, J. F., & Heaton, T. H. (2018). Deglaciation of the Pacific coastal corridor directly preceded the human colonization of the Americas. *Science Advances*, *4*(5). eaar5040. https://doi.org/10.1126/sciadv.aar5040

Letham, B., Lepofsky, D., & Greening, S. (2021). A post-glacial relative sea level curve for the central Douglas Channel area, British Columbia, Canada. *Quaternary Science Reviews*, *263*, 106991. https://doi.org/10.1016/j.quascirev.2021.106991

Letham, B., Martindale, A., Macdonald, R., Guiry, E., Jones, J., & Ames, K. M. (2016). Postglacial relative sea-level history of the Prince Rupert area, British Columbia, Canada. *Quaternary Science Reviews*, *153*, 156–191. https://doi.org/10.1016/j.quascirev.2016.10.004

Lifton, N., Sato, T., & Dunai, T. J. (2014). Scaling in situ cosmogenic nuclide production rates using analytical approximations to atmospheric cosmic-ray fluxes. *Earth and Planetary Science Letters*, *386*, 149–160. https://doi.org/10.1016/j.epsl.2013.10.052

Lowdon, J.A., & Blake, W., Jr. (1979). *Geological survey of Canada radiocarbon dates XIX* (pp. 79–87). Geological Survey of Canada Paper.

Luternauer, J. L., Conway, K. W., Clague, J. J., & Blaise, B. (1989). Late Quaternary geology and geochronology of the central continental shelf of Western Canada. *Marine Geology*, *89*(1), 57–68. https://doi.org/10.1016/0025-3227(89)90027-3

Mangerud, J., Aarseth, I., Hughes, A. L. C., Lohne, Ø. S., Skår, K., Sønstegaard, E., & Svendsen, J. I. (2016). A major re-growth of the Scandinavian Ice Sheet in Western Norway during Allerød-Younger Dryas. *Quaternary Science Reviews*, *132*, 175–205. https://doi.org/10.1016/j.quascirev.2015.11.013

Margold, M., Jansson, K. N., Kleman, J., Stroeven, A. P., & Clague, J. J. (2013). Retreat pattern of the Cordilleran Ice Sheet in central British Columbia at the end of the last glaciation reconstructed from glacial meltwater landforms. *Boreas*, *42*, 830–847. https://doi.org/10.1111/bor.12007

Margold, M., Stroeven, A. P., Clague, J. J., & Heyman, J. (2014). Timing of terminal Pleistocene deglaciation at high elevations in southern and central British Columbia constrained by ^{10}Be exposure dating. *Quaternary Science Reviews*, *99*, 193–202. https://doi.org/10.1016/j.quascirev.2014.06.027

Masson-Delmotte, V., Zhai, P., Pirani, A., Connors, S. L., Péan, C., Berger, S., et al. (2021). IPCC, 2021: Climate change 2021: The physical science basis. In *Contribution of working group I to the sixth assessment report of the intergovernmental panel on climate change*. Cambridge University Press. Retrieved from https://www.ipcc.ch/report/sixth-assessment-report-working-group-i/

Mathewes, R. W., & Clague, J. J. (2017). Paleoecology and ice limits of the early Fraser glaciation (Marine Isotope Stage 2) on Haida Gwaii, British Columbia, Canada. *Quaternary Research*, *88*(2), 277–292. https://doi.org/10.1017/qua.2017.36

McLaren, D., Fedje, D., Hay, M. B., Mackie, Q., Walker, I. J., Shugar, D. H., et al. (2014). A post-glacial sea level hinge on the central Pacific coast of Canada. *Quaternary Science Reviews*, *97*, 148–169. https://doi.org/10.1016/j.quascirev.2014.05.023

Menounos, B., Goehring, B. M., Osborn, G., Margold, M., Ward, B., Bond, J., et al. (2017). Cordilleran Ice Sheet mass loss preceded climate reversals near the Pleistocene Termination. *Science*, *358*(6364), 781–784. https://doi.org/10.1126/science.aan3001

Porter, S. C., & Swanson, T. W. (1998). Radiocarbon age constraints on rates of advance and retreat of the Puget Lobe of the Cordilleran Ice Sheet during the last glaciation. *Quaternary Research*, *50*(3), 205–213. https://doi.org/10.1006/qres.1998.2004

Potter, B. A., Baichtal, J. F., Beaudoin, A. B., Fehren-Schmitz, L., Haynes, C. V., Holliday, V. T., et al. (2018). Current evidence allows multiple models for the peopling of the Americas. *Science Advances*, *4*(8), eaat5473. https://doi.org/10.1126/sciadv.aat5473

Potter, B. A., Reuther, J. D., Holliday, V. T., Holmes, C. E., Miller, D. S., & Schmuck, N. (2017). Early colonization of Beringia and Northern North America: Chronology, routes, and adaptive strategies. *Quaternary International: The Journal of the International Union for Quaternary Research*, *444*, 36–55. https://doi.org/10.1016/j.quaint.2017.02.034

Praetorius, S. K., Condron, A., Mix, A. C., Walczak, M. H., McKay, J. L., & Du, J. (2020). The role of Northeast Pacific meltwater events in deglacial climate change. *Science Advances*, *6*(9), eaay2915. https://doi.org/10.1126/sciadv.aay2915

Seguinot, J., Khroulev, C., Rogozhina, I., Stroeven, A. P., & Zhang, Q. (2014). The effect of climate forcing on numerical simulations of the Cordilleran Ice Sheet at the Last Glacial Maximum. *The Cryosphere*, *8*(3), 1087–1103. https://doi.org/10.5194/tc-8-1087-2014

Seguinot, J., Rogozhina, I., Stroeven, A. P., Margold, M., & Kleman, J. (2016). Numerical simulations of the Cordilleran Ice Sheet through the last glacial cycle. *The Cryosphere*, *10*, 639–664. https://doi.org/10.5194/tc-10-639-2016

Shaw, J., Barrie, J. V., Conway, K. W., Lintern, D. G., & Kung, R. (2020). Glaciation of the northern British Columbia continental shelf: The geomorphic evidence derived from multibeam bathymetric data. *Boreas*, *49*, 17–37. https://doi.org/10.1111/bor.12411

Shaw, J., Stacey, C. D., Wu, Y., & Lintern, D. G. (2017). Anatomy of the Kitimat fiord system, British Columbia. *Geomorphology*, *293*, 108–129. https://doi.org/10.1016/j.geomorph.2017.04.043

Shugar, D. H., Walker, I. J., Lian, O. B., Eamer, J. B. R. R., Neudorf, C., McLaren, D., & Fedje, D. (2014). Post-glacial sea-level change along the Pacific coast of North America. *Quaternary Science Reviews*, *97*, 170–192. https://doi.org/10.1016/j.quascirev.2014.05.022

Stokes, C. R., Tarasov, L., Blomdin, R., Cronin, T. M., Fisher, T. G., Gyllencreutz, R., et al. (2015). On the reconstruction of palaeo-ice sheets: Recent advances and future challenges. *Quaternary Science Reviews*, *125*, 15–49. https://doi.org/10.1016/j.quascirev.2015.07.016

Svendsen, J. I., Briner, J. P., Mangerud, J., & Young, N. E. (2015). Early break-up of the Norwegian Channel ice stream during the last glacial maximum. *Quaternary Science Reviews*, *107*, 231–242. https://doi.org/10.1016/j.quascirev.2014.11.001

Taylor, M. A., Hendy, I. L., & Pak, D. K. (2014). Deglacial ocean warming and marine margin retreat of the Cordilleran Ice Sheet in the North Pacific Ocean. *Earth and Planetary Science Letters*, *403*, 89–98. https://doi.org/10.1016/j.epsl.2014.06.026

Walczak, M. H., Mix, A. C., Cowan, E. A., Fallon, S., Fifield, L. K., Alder, J. R., et al. (2020). Phasing of millennial-scale climate variability in the Pacific and Atlantic Oceans. *Science*, *370*(6517), 716–720. https://doi.org/10.1126/science.aba7096

Warner, B. G., Mathewes, R. W., & Clague, J. J. (1982). Ice-free conditions on the Queen Charlotte islands, British Columbia, at the height of late Wisconsin glaciation. *Science*, *218*, 675–677. https://doi.org/10.1126/science.218.4573.675

Waters, M. R. (2019). Late Pleistocene exploration and settlement of the Americas by modern humans. *Science*, *365*(6449), eaat5447. https://doi.org/10.1126/science.aat5447